Available online at **www.joac.info**

ISSN: 2278-1862

Journal of Applicable Chemistry

2019, 8 (2): 833-843

(International Peer Reviewed Journal)

Enhanced Anti-melanoma Bioefficacy of Flavonoid Loaded Gold Nanoparticles Prepared from the Plant *Madhuca longifolia* on the Mice and Human Melanoma cell lines

Saurabh Yadav[1], Mukti Sharma[1], Narayanan Ganesh[2], Shalini Srivastava[1] and ManMohan Srivastava[1]*

1. Department of Chemistry, Faculty of Science, Dayalbagh Educational Institute, Dayalbagh, Agra-282005, **INDIA**
2. Jawaharlal Nehru Cancer Hospital & Research Center, Bhopal-462001, **INDIA**

Email: dei.smohanm@gmail.com

Accepted on 8th March, 2019

ABSTRACT

The present communication warrants the potential enhancement in anti-melanoma bioefficacy of flavonoid's loaded gold nanoparticles (F@AuNp) compared to native leaf extract of the plant Madhuca longifolia. A family of four flavonoids has been ascertained in the leaves ethanolic extract of the target plant using HPLC-ESI-QTOF-MS analysis. In-vitro anti-melanoma bioefficacy has been measured against two melanoma cell lines (B16F10 and A375) using MTT bioassay. Noticeably, the native leaves extract and flavonoid's loaded gold nanoparticles did not show any toxicity towards normal lymphocyte cells highlighting their safe and non-toxic nature. Statistically significant ($p<0.05$) enhancement in the anti-melanoma bioefficacy (82.75% against B16F10) and (81.49 %) for A375 melanoma cell lines compared to native leaves extract (66.39% and 63.44%) has been successfully achieved, attaining the level near to reference drug (94.31% and 91.52%). The pathway of observed anti-melanoma efficacy of F@AuNp has been discussed based on our experimental findings on percent inhibition in mice and human melanoma cell lines, production of intercellular reactive oxygen species, release of nitric oxide, increased caspase-3 activity and melanogenesis. The native leaf extract of Madhuca longifolia and its flavonoid's loaded gold nanoparticles possess excellent prospect for the development of eccentric and complimentary herbal nanomedicine for the scaling-up the anti-melanoma bioefficacy.

Graphical Abstract

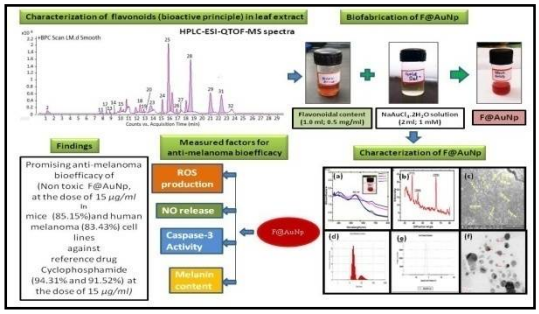

Keywords: *Madhuca longifolia*, Bioactive principle, F@AuNp, B16F10, A375 melanoma cell lines.

INTRODUCTION

Melanoma is the most destructive type of skin cancer [1] originated from melanocytes. Epidemiologic data propose that the biggest incidence is seen in the white population [2]. In the United States, 9,320 deaths have been recorded in 2018 and forecasted 91,270 new cases [3]. India has a low incidence (less than 0.5/lacs) of melanoma [4] but its increasing rate is alarming. Surgery, chemotherapy, and radiotherapy methods are used for treating skin cancer. However, these methods are not only expensive but have several limitations of recently recognized drug resistance [5]. Further, conventional drugs like (doxorubicin, dacarbazine, cyclophosphamide, 5-fluorouracil) are not highly acceptable because of their side effects like an allergic reactions, irritation, decreased red and white blood cells, and their poor responses to the patients [6]. Hence, across the globe it led to the search for novel potential compounds from the plant origin [7], which is responsible for launching a new generation of plant-derived pharmaceuticals [8]. Today, drugs from medicinal plants cabinet consist of 25% of the total drugs in developed countries and about 80% in developing countries [9]. Plant-derived drugs incorporate vinca alkaloids (vincristine, vinblastine), and taxanes (taxol, docetaxel) have anticancer nature [10]. Nanobiotechnology has been found significant as site-specific tumour therapy, radiotherapy, gene therapy, as well as chemotherapy. In the latest perspectives, nanoparticles surrounded with medicinally important phytoconstituents have occupied a vital position in designing and manufacturing of nano-medicines [11-15].

Recent realization that the plants having particular bio-efficacy should be explored and enhanced for other bonafide activities has motivated us to enhance anti-inflammatory [16] and wound healing [17] bio-efficacies using seed of the plant *Madhuca longifolia.* In continuation of our work exploring anti-melanoma bioefficacy in the bark of the plant *Madhuca longifolia* [18], the present communication reports our endeavors' on the green synthesis and characterization of flavonoids loaded gold nanoparticles (F@AuNp) exploring equally good anti-melanoma bioefficacy in leaf extract of the same plant. *In-vitro* anti-melanoma bio-efficacy of F@AuNp has been assessed against mice (B16F10) and human (A375) melanoma cell lines using MTT bioassay using reference drug (cyclophosphamide). *Madhuca longifolia* commonly known as Mahua is one of the most important wildly distributed Indian forest plants and belonging to the family Sapotaceae. The different parts of the plant are used in traditional and folk remedy in the various ailments in rural and tribal areas [19-21].

MATERIALS AND METHODS

Extraction of plant material: The fresh leaves of *M. longifolia* were collected from the village Rajaborari (Madhya Pradesh) and verified by Taxonomy Division, Department of Botany, Dayalbagh Educational Institute, Dayalbagh, Agra, India, where a sample was deposited with the voucher specimen number DEI/DB/DH/2015-074. The leaves were cleaned, shade dried and ground into powder form. Microwave-assisted extraction of the chlorophyll free leaves was carried out in aqueous alcoholic solution at 200W for 5 minutes. The filtrate was subjected to rota-vapour distillation and finally dried by purging nitrogen. Sodium tetrachloroaurate dihydrate ($NaAuCl_4.2H_2O$), 3-(4, 5 dimethylthiazol-2-yl)-2,5-diphenyltetrazolium bromide (MTT) reagent and other solvents were purchased from Sigma Aldrich, USA. All experiments were performed using double distilled water as a medium.

Phytochemical investigations: The dried mass fraction (10 gm) was subjected to column chromatographic separation [length 120 cm; diameter 4 cm; mesh 60; stationary phase; silica gel (125gm)] and eluted with CH_3OH:$CHCl_3$ (3:7). After the removal of solvent, a light brown mass was obtained. This brown mass fraction was subjected to HPLC-ESI-QTOF-MS mass spectra for the characterization of the flavonoids. HPLC-MS analysis was performed on quadrupole time-of-flight (QTOF) mass spectrometer connected with Agilent 1200-HPLC system via dual electrospray ionization interface (Agilent Technologies, USA). HPLC separation was carried out on a Poroshell

120 EC-C18 column (50mm× 4.6mm, 2.7 µ). The mobile phase consisted of (0.1%) formic acid solution (A) and methanol (C) with flow rate of (0.5 ml/min) under the gradient program of 30 to 90% (C) for initial 10 min, then 90% (C) from 10 to 20 min, 90 to 30% (C) from 20 to 25 min, 30% (C) from 25 to 30 min. The mass spectrometric analysis was performed in positive ESI mode. The resolving power of the QTOF analyzer was set above 10,000 (FWHM). The spectra's were acquired within a mass range of *m/z* 100-1500. Capillary temperature was set to 350°C, N_2 nebulizer pressure (40 psi) and gas flow rate (10 L min^{-1}). HPLC-ESI-QTOF-MS spectra decorated the existence of four important flavonoids.

Green synthesis of flavonoids loaded gold nanoparticles (F@AuNp): The fabrication of F@AuNp was carried out at different pH, varying the concentration of $NaAuCl_4.2H_2O$ solution, and flavonoidal content constant. Optimized experimental conditions of the fabrication of nanoparticles were as follows: flavonoidal content (1.0 mL; 0.5 mg mL^{-1}), was mixed with sodium tetrachloroaurate dihydrate solution (2 mL; 1 mM) at pH (2, 4, 8 and 10) and sonicated (15 min; 20 KHz) at room temperature. The formation of flavonoids loaded gold nanoparticles (F@AuNp) were observed by a change in colour from pale yellow to ruby red.

Characterization of F@AuNp: The bio-fabricated F@AuNp was characterized for optical properties with the help of UV-Visible spectrophotometer, (Lab India, India). The X-ray diffraction pattern of F@AuNp was recorded using XRD (Bruker AXS D8 Advance, Germany) over 20^o-80^o with scan run 40 min^{-1}, step size of 0.02^o and Cu Kα radiation of λ= 1.54Å. The accurate physical size of F@AuNp was measured using High Resolution Transmission electron microscopy (HR-TEM; Tecnai G2 T 20 ST, Germany). The hydrodynamic size distribution with poly-dispersity index (PDI) and their zeta potential was analyzed using zeta sizer (Nano ZS90 model Malvern, Germany).The morphology and elemental composition of F@AuNp were studied using FE-SEM (Nova Nano FE-SEM 450, Netherland) and EDX (Tecnai G2 T 20 ST, Germany) techniques respectively.

Cell culture: The mice (B16F10) and human (A375) melanoma cell lines were purchased from National Centre for Cell Science, Pune, India, and grown-up in Dulbecco's Modified Eagle's Medium (DMEM) containing antibiotics, L-glutamine (2 mM), fetal bovine serum (10%). Cells were kept at 37°C, with relative humidity (100%), CO_2 (5%), and air (95%). The culture medium was changed thrice in a week. The single cell suspension was made using trypsin-ethylene di-amine tetra acetic acid. The cell suspension was diluted with media containing FBS (5%) to obtain final density ($1x10^5$cells mL^{-1}). 96 well plates were seeded with (10,000 cells $well^{-1}$) and incubated in the CO_2 incubator. The cells were treated (in triplicate) with different concentrations of the test samples after 24 h against control. The standard chemotherapeutic drug (cyclophosphamide), frequently used for the treatment of melanoma cancer, was used as a reference drug.

Isolation of human lymphocytes: Blood samples (5 mL) were collected from five healthy persons by vein-puncture in a heparin-coated vacutainer [22]. Defibrinated blood (2 mL) and Ficoll-Paque PLUS (2.5 mL) were mixed and centrifuged for 30 min and upper layer was removed leaving the lymphocyte layer undisturbed at the interface. The lymphocyte layer was transferred to a clean tube and further centrifuged for 30 min. The balanced salt solution was added and centrifuged again. The supernatant was discarded and suspension of the lymphocytes was mixed with RPMI-1640 medium. Few drops of PHA (mitogen) were added and incubated for 24 h in a CO_2 incubator. Ethical committee of Jawaharlal Nehru Cancer Hospital and Research Centre, Bhopal, India had approved this work.

Intracellular reactive oxygen species (ROS) generation: Mice melanoma cell lines were treated with (20 µL) of experimentally measured IC_{50} of F@AuNp (12.82 µg mL^{-1}) and incubated for 24 h. The cells were washed with fresh media and incubated with developing agent (DCF) 2, 7 Di Chloro Dihydro Fluorescein Diacetate (1 µg mL^{-1}) for 30 min at 37°C. DCF fluorescence was used to determine excitation at (485 nm) and emission at (520 nm) using a Cary Eclipse Fluorescence Spectrophotometer [23].

Nitric oxide release assay: Serum (50 µL well^{-1}) was treated with (20 µL) of experimentally measured IC_{50} of F@AuNp (12.82 µg mL^{-1}) and incubated for 24 h. Griess reagent (100 µL) was added and incubated at room temperature for 10 min. Absorbance was recorded at 550 nm against calibration curve of sodium nitrite. The level of nitric oxide was expressed as µM mg^{-1} protein [24].

Caspase-3 activity: Caspase-3 activity in melanoma cells was performed using a colorimetric caspase-3 assay kit [25]. The monolayer cell culture was trypsinized and the cell count was adjusted ($2x10^5$ well^{-1}) using a medium containing 10% fetal bovine serum (FBS). To each well of 96-well plates, diluted cell suspension (2 mL) was added. After 24 h when a partial monolayer was formed, the supernatant was flicked off, washed, treated with different concentrations of F@AuNp (0, 25, 50, 75, and 100 µg mL^{-1}) and PBS-DMEM (10%). Caspase-3 levels were measured using ELISA readers at λ_{max} 450 nm and the desired activity was calculated as fold increase over control sample.

Melanin content assay: Mice melanoma cells were seeded with ($2x10^5$ cells well^{-1}) in a 6-well culture (2 mL) plates and incubated overnight to allow cells to adhere. The cells were exposed to various concentration of the extract for 72 h, the cells were washed with PBS and lysed with NaOH (1N; 800 µL) containing DMSO (10%) for 1 h at 75°C. The melanin content was determined using a microplate reader at 405 nm absorbance [26].

RESULTS AND DISCUSSION

HPLC-ESI-QTOF-MS profile: HPLC-ESI-QTOF-MS chromatogram (Figure 1) ascertained the existence of a family of four flavonoids namely: Quercetin (11), 3, 6 Dihydroxy flavones (15), Di-hydroquercetin (23) and Di-hexosyl-quercetin (32) at retention time 7.6 min, 10.1 min, 13.9 and 23.6 min respectively. Recording of QTOF-MS spectra, based on observed mass, accurate mass of the molecules ascertained compound (11) as Quercetin; m/z 303.05, (15) as 3,6 Dihydroxy flavones; m/z 323.14, (23) Di-hydroqucertein; m/z 301.21 and (32) as Di-hexosyl-quercetin; m/z 621.31. Other peaks were corresponding to stigmasterol; m/z 413.39 (18), lucien; 131.17 (19), oleanolic acid; 457.36 (24), palmitic acid; 257.24 (27), along with some unidentified peaks.

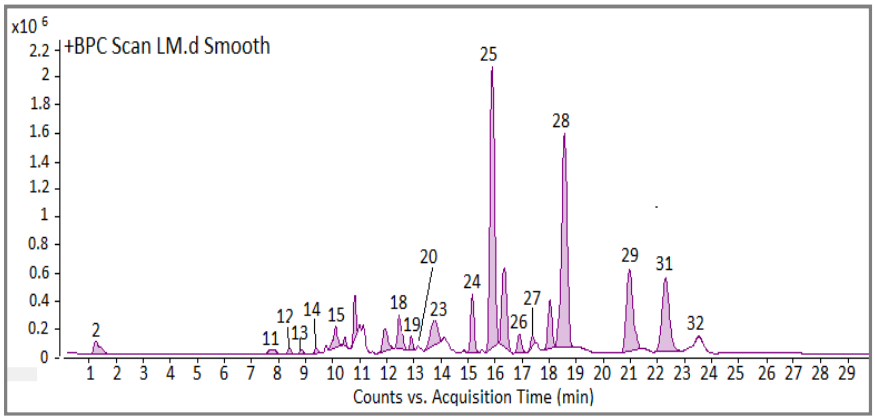

Figure 1. HPLC-ESI-QTOF-MS chromatogram depicting the presence of flavonoids.

Flavonoidal compounds have been reported active for the adequate antioxidant potential [27-29]. Antioxidants, as immunity boosters, have also been proved to strengthen the anticancer activity by several mechanisms [30, 31]. The plant *M. longifolia* (leaf) has been ascertained to possess a family of four flavonoids. The strong synergistic reduction potential of flavonoids in the target plant (leaves) was used for the fabrication of F@AuNp and explored for anti-melanoma bioefficacy against mice (B16F10) and human (A375) melanoma cell lines. The mechanistic pathway of flavonoids in the fabrication of F@AuNp has been discussed in our earlier paper [18].

Ultraviolet-Visible spectrophotometer: The synthesis of F@AuNp was carried out at different concentrations (10^{-4}-10^{-2}M) of $NaAuCl_4.2H_2O$, keeping the concentration of extracted flavonoid constant (2 mL; 0.5mg mL^{-1}). At higher concentration (10^{-2} M) of $NaAuCl_4.2H_2O$, no perceptible Surface Plasmon Resonance (SPR) peak appeared in the desired range of 500-550 nm. At dilute concentrations of $NaAuCl_4.2H_2O$ (10^{-3} and 10^{-4} M), SPR peaks were found at 542 and 536 nm respectively. The absorbance of SPR peak of $NaAuCl_4.2H_2O$ at (10^{-3} M) concentration was of much higher intensity and, therefore, considered optimum concentration for the synthesis of F@AuNp. Any further dilution depicted marked decrease in intensity of desired peak. F@AuNp was fabricated in the pH range (2-10). At highly acidic and basic conditions, no desirable SPR peaks were obtained. The pH 4 was found optimum for the formation of gold nanoparticles, depicting SPR peak (λ_{max}) at 542 nm (Figure 2). F@AuNp exhibited fabulous stability over four weeks at pH 4.

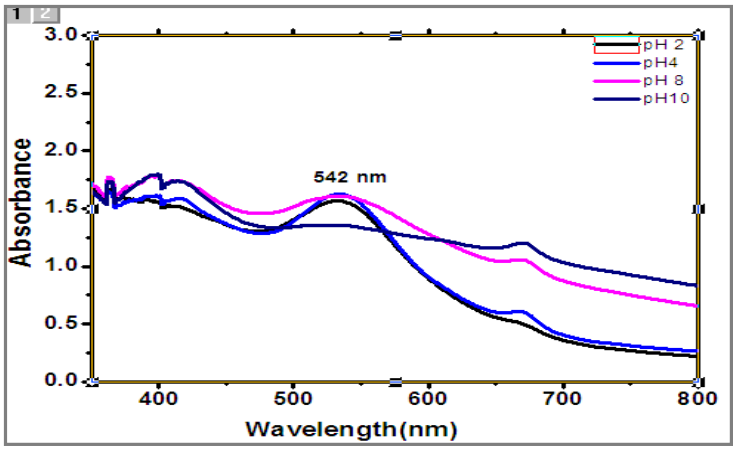

Figure 2. UV-vis spectra of F@AuNp at different pH.

X-Ray diffraction: Bragg diffraction peaks appeared positions 2θ at 38.2°, 44.5°, and 64.7° in the bio-fabricated F@AuNp (Figure 3). It could be indexed to (111), (200) and (220) having lattice planes of face-centre cubic compared with (JCPDS file 04-0784). The intensity of the diffraction peaks (200) and (220) was found lower than corresponding crystallographic planes (111). The fact established that lattice plane (111) is the transcendent crystallographic plane and is more reactive because of its high atom density [32]. The observed noise and broadening of the peak in XRD record of F@AuNp may be assigned to the existence medicinally important secondary metabolites (flavonoids) loaded on the surface of fabricated F@AuNp.

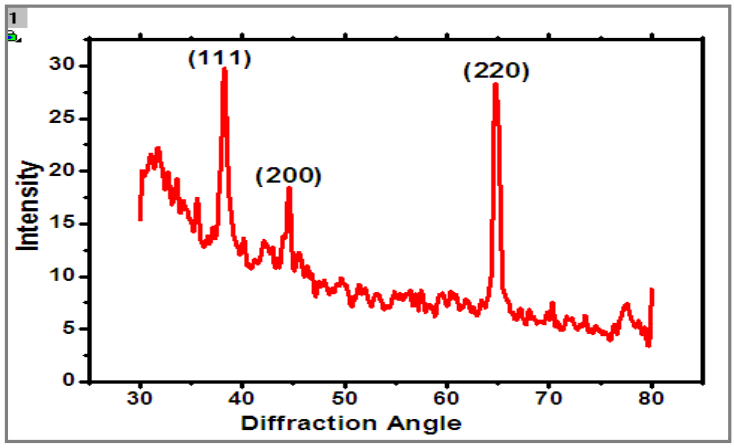

Figure 3. X-Ray diffraction pattern of F@AuNp

FE-SEM and EDX studies: FE-SEM images (Figure 4a) acquired from drop-coated films of nanoparticles indicated poly dispersed, cube, triangular and spherical shaped morphology of bio-fabricated gold nanoparticles. The desirable signals of the metal (Au) were found in EDX spectra of the F@AuNp (Figure 4b). However, the presence of other peaks of Cu which is an artifact of the Cu-grid on which the sample was coated and the peaks of C, O and N might have initiated from the bio-molecules that are adhered on to the surface of nanoparticles.

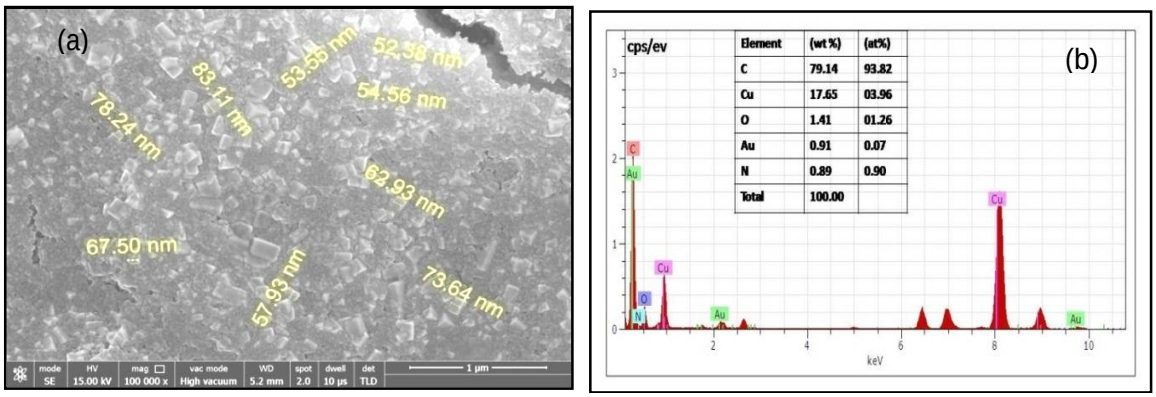

Figure 4. (a) FE-SEM image, **(b)** EDX spectra of F@AuNp.

HR-TEM and Dynamic light scattering: HR-TEM analysis confirmed the formation of F@AuNp in the size range (9.66-17.58 nm) at the magnification of 300,000X (Figure 5a). A HR-TEM image of nanoparticles exhibited light-coloured shaded coating around the nanoparticles; again provide support to the loading of flavonoids on the nanoparticles. The dynamic light scattering (DLS) spectrum highlighted asymmetric distribution range of nanoparticles mainly in the range (4 to 100 nm) with poly-dispersive index 0.358; intercept 0.678 (Figure 5b). However, the very little population was extended in the range of 200 nm. It also provided the average hydrodynamic size (Z-Average) of F@AuNp (17.58 nm). Zeta potential of F@AuNp, determined in water medium as a dispersant was-25.7 mV (Figure 5c). The magnitude of observed high negative charge on the bio-fabricated nanoparticles might be acting as a repulsive barrier, avoiding aggregation of nanoparticles. The fact also supports the HR-TEM observation indicating light coloured shade coating around the nanoparticles. HR-TEM provides the accurate size of nanoparticles but DLS delivers important information regarding the size distribution of particles. The difference possibly reflect the fact that, HR-TEM only measures the physical size while DLS measures the hydrodynamic size of the particles along with the ions, attached to the surface and move with the nanoparticles in solution [33].

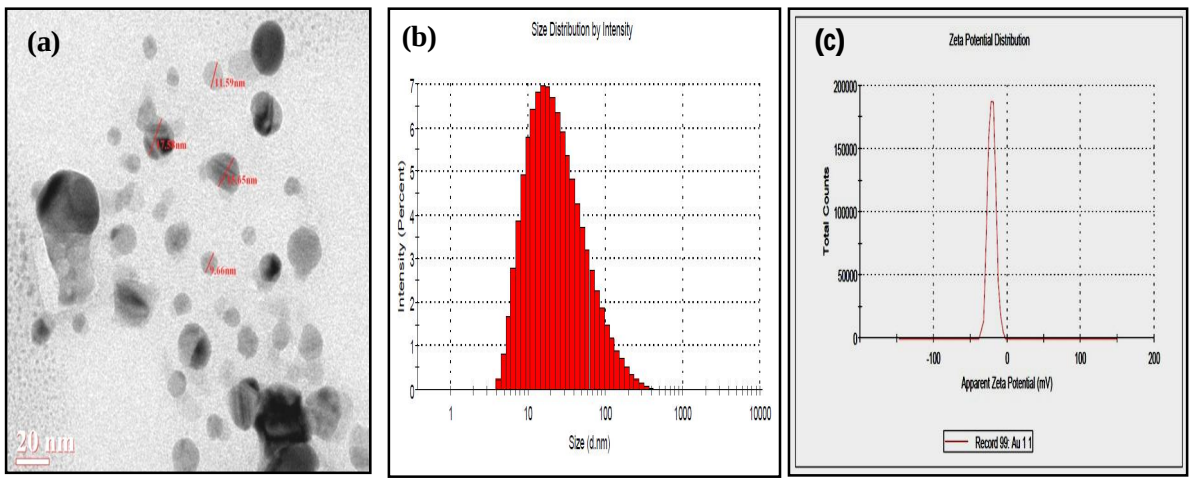

Figure 5. (a) HR-TEM image of F@AuNp, **(b)** &**(c)** Particle size distribution and zeta potential of F@AuNp.

In-vitro anti-melanoma activity: Anti-melanoma activity (in terms of percent inhibition) was measured in all the treatment groups, control, and reference drug using MTT bioassay (Table 1).

Table 1. *In-vitro* percent inhibition in MTT bioassay on mice (B16F10) and human (A375) melanoma cell line

Groups	Doses (µg mL^{-1})	% Inhibition	
		B16F10	A375
Control		1.25±0.45	1.89±0.97
Reference Drug (Cyclophosphamide)	**10**	67.36±1.11	62.53±1.56
	15	94.31±1.21	91.52±1.54
	20	97.13±1.01	93.77±1.48
Leaf extract	**25**	45.34±1.10	46.14±1.31
	50	66.39±1.12	63.44±1.14
	100	67.92±1.25	64.32±1.15
Flavonoidal content	**10**	62.12±1.21	60.93±1.32
	15	77.14±1.22	75.37±1.45
	20	78.42±1.10	76.19±1.14
F@AuNp	**10**	71.71±1.12	70.12±1.41
	15	82.75±1.21	81.49±1.19
	20	84.03±1.51	84.19±1.15

Each value is mean ± SD (n=3) p<0.05, significant, compare to control

A perusal of the table 1 demonstrates that in the entire groups statistically significant enhancement in the percentage inhibition occurred in a dose dependent manner. Increased percentage inhibition (10.75-11.93%) of the target bioefficacy in the case of flavonoidal treatment compared to leaf extract at a drastically reduced dose (15 µg mL^{-1}) signified the role of flavonoids as the feasible bioactive constituent of the leaf extract of the plant *M. longifolia*. Further, F@AuNp exhibited an additional increase of (5.61%) in anti-melanoma bioefficacy compared to flavonoids. The fact supports the school of thoughts that bioactive principle loaded gold nanoparticles impart significant enhancement in the bioefficacy [**34, 35**]. The observed significant enhancement in anti-melanoma bioefficacy has been ascribed to the biocompatibility, astonishing optical properties, high surface area to volume ratio (nano sizing), and coating of medicinally important flavonoidal content on the nanoparticles. The oxidized flavonoids (quinone moiety) being electron deficient may also impart free radical scavenging ability, thus adding additional antioxidant properties.

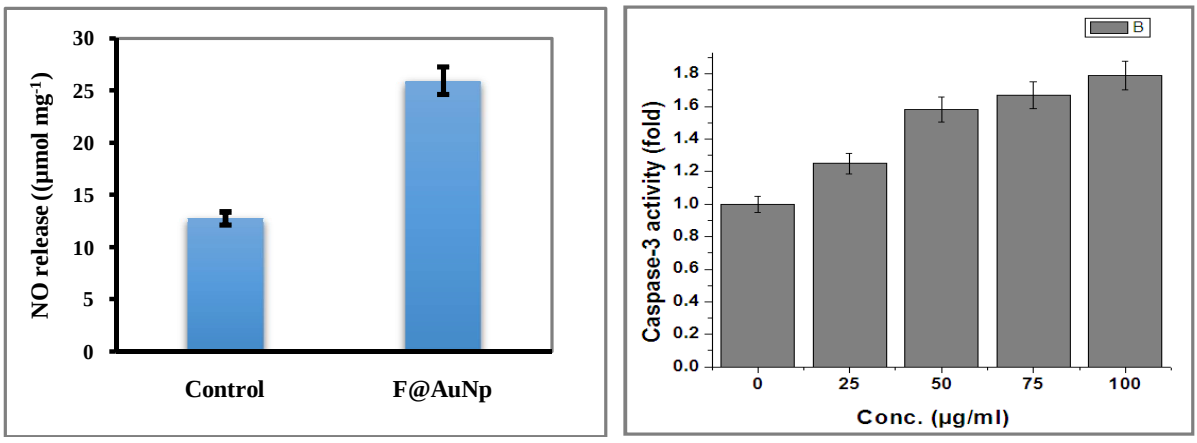

Figure 6. (a) Nitric oxide (NO) release level, **(b)** Caspase-3 activity of F@AuNp.

Overall improved permeability in the cell membrane of cancerous cell could largely inhibit the proliferation of the cancerous cell. The facts find support from our further *in-vitro* cellular apoptosis studies. The elevation *(p<0.05)* in the level of intracellular reactive oxygen species (55.32%) and production of serum NO level (66.83 %) against control (Figure 6a) are the indications of the

enhanced oxidative stress in F@AuNp treatment. ROS, play a dual character in living systems. The moderate concentration of ROS can promote cell proliferation, while excessive amount results into cellular apoptosis via oxidative damage to lipids, proteins, and DNA. Nitric Oxide reacts with superoxide to produce toxic peroxynitrite ($ONOO^-$) anion, which imparts anti-tumour activity [**36**]. In addition, observed rise in caspase-3 activity (Figure 6b) with the go-up in the concentration of F@AuNp signifies the trend of quick cell wall disruption, shrinking and rupturing of the cells. Caspase enzymes are mainly involved in the apoptotic cascade and lead to proteolysis of specifically coupled with involuntary cell death. The caspase-3 activity involves a variety of functions including activation of a cytosolic endonuclease as well as deoxyribonuclease enzyme that cleavage genomic DNA into oligonucleosomal fragments [**37, 38**].

Melanogenesis is a complex process liable for the mammalian colour of skin governed by various enzymatic processes [**39, 40**]. It involves a series of redox reactions controlling the production of toxic mutagenic and ROS compounds. Reactive Oxygen Species cause into decreased enzymatic antioxidant effect with extensive normal melanocytes damage. Therefore, regulation of melanogenesis with increased antioxidant status can be an effective strategy to achieve anti-melanogenesis. Our experimental findings showed that bio-fabricated F@AuNp did not show any significant decrease (Figure 7) in the production of melanin content in the concentration range (0.001 to 0.125mg mL^{-1}), highlighting no inhibitory effects. A number of flavonoids present in the leaf extract of *M. longifolia* governed the regulation of melanin biosynthesis [**41, 42**]. The finding suggested that F@AuNp has favorable melanogenesis property.

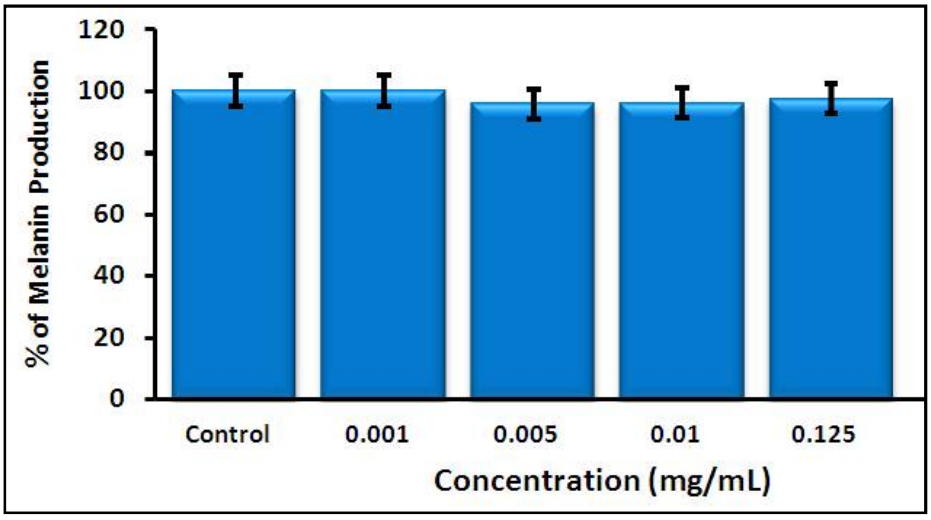

Figure 7. The effect of various concentrations of F@AuNp on melanin content in B16F10 cell line.

APPLICATION

This study explored a noticeable anti-melanoma prospective of ethanolic leaf extract of the plant *Madhuca longifolia* and enhancement in the target bioefficacy through its flavonoids loaded gold nanoparticles. These findings suggested that the plant *Madhuca longifolia* and its bioactive principle loaded gold nanoparticles seem to be an ultimate candidate for the development of herbal nanomedicine for the treatment of melanoma.

CONCLUSION

The present communication explores significant anti-melanoma bioefficacy (66.39%) in the native leaf ethanolic extract of *M. longifolia.* The excellent enhancement in target anti-melanoma bioefficacy

(82.75%) was obtained using the flavonoids loaded gold nanoparticles (F@AuNp). The inherent medicinal property of gold, large surface area of nanoparticles, difference in zeta potential value of F@AuNp vs cell membrane, simultaneous loading of flavonoids as an anti-cancer agent has been assigned to the enhanced anti-melanoma bioefficacy of F@AuNp. The leaf of *M. longifolia* seems to be an ideal candidate for the development of complementary herbal nano-medicine for treatment of melanoma cancer. The detailed work on anti-melanoma activity of the plant *M. longifolia* and *in-vivo* experiments are in progress.

ACKNOWLEDGEMENTS

The authors gratefully acknowledge Prof. P. K. Kalra, Director, Dayalbagh Educational Institute and Prof. Sahab Dass, Head, Department of Chemistry, Dayalbagh Educational Institute, Dayalbagh, Agra for providing necessary facilities and motivation to carry out the research.

Ethics approval and consent to participate: Ethical committee of Jawaharlal Nehru Cancer Hospital and Research Centre, Bhopal, India had approved this work.

Funding: This work was supported by the University Grants Commission, New Delhi for providing Basic Scientific Research Fellowship to one of the author Saurabh Yadav [UGC-BSR; F-25-1/2014-15(BSR)/07-191/2007].

REFERENCES

[1]. J. Chen, R. Shao, X. D. Zhang, C. Chen, Applications of Nanotechnology for Melanoma Treatment, Diagnosis, and Theranostics, *International Journal of Nanomedicine,* **2013**, 8, 2677-2688. DOI: 10.2147/IJN.S45429.

[2]. E. D. Vriesa, M. Sierraa, M. Piñerosa, D. Loriad, D. Forman, The burden of cutaneous melanoma and status of preventive measures in Central and South America, *Cancer Epidemiology*, **2016**, 44S, S100–S109. DOI: 10.1016/j.canep.2016.02.005.

[3]. R. L. Siegel, K. M. Miller, A. Jemal, Cancer Statistics, *A Cancer Journal for Clinicians*, **2018**, 68(1) ,7- 30.

[4]. C. R. Lakhtakia, C. A. Mehta, S. K. Nema, Melanoma: A Frequently Missed Diagnosis, *Medical Journal Armed Forces India*, **2009**, 65, (3) 292- 294.

[5]. M. Chidambram, R. Manavalan, R. Kathiresan, Nanotherapeutics to Overcome Conventional Cancer Chemotherapy Limitations. *Journal of Pharmacy and Pharmaceutical Sciences*, **2011**, 14 (1), 67-77.

[6]. K. H. Khan, R.B.Goody, H. Hameed, A. Jalil, V. M. Coyle, Mc, J. J. Aleer, Metastatic Melanoma: A Regional Review and Future Directions. *Tumori Journal*, **2012**, 98(5), 575-580.

[7]. Y. Haidan, M. Qianqian, Y. Li, P. Guangchun, Review: The Traditional Medicine and Modern Medicine from Natural Products. *Molecules*, **2016**, 21(5), 559-579.

[8]. M. Raj, S. Padhi, J.F. Gmel, Biochemical and Antioxidant Analysis of *Madhuca Indica*, *Scholarly Research Journal for Interdisciplinary Studies*, **2015**, 3(16), 2657-2666.

[9]. M. A. Qazi, K. Molvi, Herbal medicine: A Comprehensive Review, *International Journal of Pharmacy Science and Research*, **2016**, 8(2), 1-5.

[10]. M. Moudi, R. Go, S.Y.C. Yien, M. Nazre, Vinca Alkaloids, *International Journal* of *Preventive Medicine,* **2013**, 4(11), 1231-1235.

[11]. K. Katti, N. Chanda, R. Shukla, A. Zambra, T. Subramanians, R. Kulkarni, R. Kannan, V. K. Katti, Green Nanotechnology from Cumin Phytochemicals: Generation of Biocompatible Gold Nanoparticles, *International Journal of Green Nanotechnology: Biomedicine*, **2009**, 1(1) B39-B52.

[12]. S. D. Brown, P. Nativo, J. A. Smith, D. Stirling, P. R. Edwards, B. Venugopal, D. J. Flint, J. A. Plumb, D. Grahams, N. J. Wheate, Gold Nanoparticles for the Improved Anticancer Drug

Delivery of the Active Component of Oxaliplatin, *Journal of American Chemical Society,* **2010**, 132(13), 4678-4684.
[13]. M. Khoobchandani, A. Zambre, K. Katti, C. H. Lin, V. K. Katti, Green Nanotechnology from Brassicaceae: Development of Broccoli Phytochemicals-Encapsulated Gold Nanoparticles and Their Applications in Nanomedicine, *International Journal of Green Nanotechnology*, **2013**, 1, 1-15. DOI: 10.1177/194308921350947.
[14]. A. M. Gamal-Eldeena, D. Moustafac, S. M. El-Dalya, M. A. M. Abo-Zeida, S. Saleh, M. Khoobchandani, K. Katti, R. Shukla, V. K. Katti, Gum Arabic-encapsulated Gold Nanoparticles for a Non-invasive Photothermal Ablation of Lung Tumor in Mice, *Biomedicine and pharmacotherapy*, **2017**, 89, 1045-1054. DOI: 10.1016/j.biopha.2017.03.006.
[15]. D. N. Navale, P. Kalambate, P. B. Ranade, D. K. Kulal, S.W. Zote, Green Synthesis of Gold Nanoparticles using Crinum asiaticum Leaf Extract and their Application in Size Dependent Catalytic Activity, *J. Applicable Chem.*, **2018**, 7(5), 1285-1290.
[16]. M. Sharma, S. Yadav, M. M. Srivastava, N. Ganesh, S. Srivastava, Promising Anti-inflammatory Bio-efficacy of Saponin Loaded Silver Nanoparticles Prepared from the Plant *Madhuca longifolia. Asian Journal of Nanoscience and Materials*, **2018**, 1(4), 244-261.
[17]. M. Sharma, S. Yadav, M.M. Srivastava, N. Ganesh, S. Srivastava, Biofabrication, and characterization of favonoid-loaded Ag, Au, Au–Ag bimetallic nanoparticles using seed extract of the plant *Madhuca longifolia* for the enhancement in wound healing bio-efficacy's, *Progress in Biomaterials*, **2018**, http://doi.org/10.1007/s40204-019-0110-0.
[18]. S. Yadav, M. Sharma, N. Ganesh, S. Srivastava, M. M. Srivastava, Bioactive Principle Loaded Gold Nanoparticles as Potent Anti-melanoma Agent: Green Synthesis, Characterization and *In-vitro* Bioefficacy, *Asian Journal of Green Chemistry*, **2019**, DOI: 10.22034/ ajgc. 2019. 150792. 1107.
[19]. K. N. Akshatha, S. M. Murthy, N. Lakshmidevi, Ethnomedical uses of *Madhuca longifolia*-A Review, *International Journal of Life science and Pharma Research*, **2013**, 3(1), 44-53.
[20]. M. F. Ramadan, A. A. A. Mohdaly, A. M. A. Assiri, M. Tadros, B. Niemeyer, Functional Characteristics, Nutritional Value and Industrial Applications of *Madhuca longifolia* seeds: An overview, *Journal of Food Science and Technology*, **2016**, 53(5), 2149-2157.
[21]. P. S. Jerine, S. E. Prince, Diclofenac-induced Renal Toxicity in Female Wistar Albino Rats is protected by the Pre-treatment of Aqueous Leaves Extract of *Madhuca longifolia* through suppression of Inflammation, Oxidative Stress, and Cytokine Formation. *Biomedicine and Pharmacotherapy*, **2018**, 98, 45-51. DOI: 10.1016/j.biopha.2017.12.028
[22]. S. Madhe, P. Bansal, M. M. Srivastava, Enhanced antioxidant activity of gold nanoparticles loaded 3, 6-dihydroxyflavone: A Combinational Study, *Applied Nanoscience*, **2014**, 4, 153-161. DOI: 10.1007/s13204-012-0182-9.
[23]. L. Hudson, F. Hay, Practical immunology, 3rd ed., Blackwell, Oxford Kerr MA, Thorpe R (eds.) (**1994**) Immunochemistry Labfax. Academic Press, Oxford.
[24]. G. Giovannoni, J. M. Land, G. Keir, E. J., Thompson, S.J. R. Heales, Adaptation of the Nitrate Reductase and Griess Reaction Methods for the Measurement of Serum Nitrate Plus Nitrite Levels, *Annals of Clinical Biochemistry*, **1997**, 34, 193-198. DOI: 10.1177/00045632970340 0212.
[25]. S. K. Mahapatra, S. P. Chakaraborty, S. Das, S. Roy, Methanol extract of *Ocimum gratissimum* protects Murine Peritoneal Macrophages from Nicotine Toxicity by Decreasing Free Radical Generation, Lipid and Protein Damage and Enhances Antioxidant Protection. *Oxidative medicine and cellular longevity*, **2009**, 2(4), 222-230.
[26]. Y. Y. Chan, K. H. Kim, S. H. Cheah, Inhibitory effects of *Sargassum Polycystum* on Tyrosinase Activity and Melanin Formation in B16F10 Murine Melanoma Cells, *Journal of Ethno pharmacology*, **2011**, 137(3), 1183-1188.
[27]. J. Zhishen, T. Mengcheng, W. Jianming, The Determination of Flavonoids Content in Mulberry and their Scavenging Effects on Superoxide Radicals, *Food Chemistry*, **1999**, 64(4), 555-559.
[28]. W. Zheng, S. Y. Wang, Antioxidant Activity, and Phenolic Compounds in Selected Herbs, *Journal of Agricultural and Food Chemistry*, **2001**, 49, (11) 5165-5170.

[29]. T. S. Inganakal, M. L. Ahmed, P. Swamy, Neuropharmcological Potential of Methanolic Extract and a Triterpene Isolated from *Madhuca longifolia* Leaves in Mice, *Indian Journal of Experimental Biology,* **2012**, 50(12), 862-866.
[30]. R. K. Sharma, S. Gulati, S. Mehta, Preparation of Gold Nanoparticles Using Tea: A Green Chemistry Experiment, *Journal of Chemical Education,* **2012**, 89(10), 1316-1318.
[31]. K. B. Panday, S. I. Rizvi, Plant Polyphenols as Dietary Antioxidants in Human Health and Disease. *Oxidative Medicine and Cellular Longevity*, **2009**, 2(5), 270-278.
[32]. G. Zhang, M. Du, X. Li, J. Huang, X. Jiang, D. Sun, Green Synthesis of Au–Ag Alloy Nanoparticles Using *Cacumen platycladi* Extract *RSC Advances*, **2013**, 3(6), 1878-1884.
[33]. P. C., Lin, S. Lin, P. C. Wang, R. Sridhar, Techniques for physicochemical characterization of nanomaterials, *Biotechnology Advances*, **2014**, 32(4), 711-726.
[34]. S. Velavan, A. Amargeetha, X-ray Diffraction (XRD) and Energy Dispersive Spectroscopy (EDS) Analysis of Silver Nanoparticles Synthesized from *Erythrina indica* Flowers, *Journal of Nanoscience and Technology*, **2018**, 5(1), 1-5.
[35]. J. Kim, J. Kim, J. S. Bae, ROS Homoeostasis and Metabolism: A Critical liaison for Cancer Therapy, *Experimental and Molecular Medicine*, **2016**, 48(11), 1-13.
[36]. S. Habib, A. Ali, Biochemistry of Nitric Oxide. *Indian Journal of Clinical Biochemistry*, **2011**, 26(1), 3-17.
[37]. E. A. Slee, C. Adrain, S. J. Martin, Executioner Caspase-3, 6, and 7 perform distinct, Non-redundant Roles During the Demolition Phase of Apoptosis, *Journal of Biological Chemistry*, **2001**, 276(10), 7320-7326.
[38]. A. B. Parrish, C. D. Freel, S. Kornbluth, Cellular Mechanisms Controlling Caspase Activation and Function. *Cold Spring Harbor Perspective in Biology*, **2013**, 5(6), 1-25.
[39]. A. Slominski, B. Zbytek, R. Slominski, Inhibitors of Melanogenesis Increase Toxicity of Cyclophosphamide and Lymphocytes against Melanoma cells, *International Journal of Cancer*, **2009**, 124(6), 1470-1477.
[40]. Y. T. Tsao, Y. F. Huang, C. Y. Kuo, Y. C. Lin, W. C. Chiang, W. K. Wang, Hinokitiol Inhibits Melanogenesis via AKT/mTOR Signaling in B16F10 Mouse Melanoma Cells, *International Journal of Molecular Science*, **2016**, 17, (2) 248-255.
[41]. Z. Qiao, Y. Koizumi, M. Zhang, M. Natsui, M. J. Flores, L. Gao, Anti-Melanogenesis Effect of *Glechoma hederacea* L. Extract on B16 Murine Melanoma Cells, *Bioscience, Biotechnology, and Biochemistry*, **2012**,76(10), 1877-1883.
[42]. Y. C. Huang, C. H. Yang, Y. L. Chiou, Citrus Flavanone Naringenin Enhances Melanogenesis through the Activation of Wnt/β-catenin Signalling in Mouse Melanoma Cells, *Phytomedicine*, **2011**, 18, (14)1244-1249.